

Ferrocenyl Diphosphines Containing Stereogenic Phosphorus Atoms. Synthesis and Application in the Rhodium-Catalyzed Asymmetric Hydrogenation

Francesca Maienza, Michael Wörle,[†] Pascal Steffanut,[‡] and Antonio Mezzetti*

Laboratorium für Anorganische Chemie, ETH-Zentrum, CH-8092 Zürich, Switzerland

Felix Spindler

Scientific Services, Novartis Services Ltd, CH-4002 Basle, Switzerland

Received September 7, 1998

Enantiomerically pure (*R*)-2-methoxyphenyl(phenyl)-*O*-methylphosphinite borane (**1a**) and (*R*)-1-naphthyl(phenyl)-*O*-methylphosphinite borane (**1b**) react with 1,1'-dilithioferrocene to give (*S,S*)-1,1'-bis(2-methoxyphenyl(phenyl)phosphino)ferrocene borane (**2a**) and (*S,S*)-1,1'-bis(1-naphthyl(phenyl)phosphino)ferrocene borane (**2b**). Deboronation with morpholine yields the diphosphines (*S,S*)-1,1'-bis(2-methoxyphenyl(phenyl)phosphino)ferrocene (**3a**) and (*S,S*)-1,1'-bis(1-naphthyl(phenyl)phosphino)ferrocene (**3b**) in high yields and high diastereo- and enantiomeric purity, as determined on the corresponding phosphine oxides **4a,b**. X-ray investigations support the (*S,S*) configuration of **2a** and disclose the coordination properties of **3a** in the platinum derivative [PtCl₂(**3a**)] (**5a**). The rhodium(I) derivatives [Rh(COD)-(**3a,b**)]BF₄ (**6a,b**) have been prepared and tested in the enantioselective catalytic hydrogenation of various olefins and ketones. Excellent enantioselectivity is achieved in the asymmetric hydrogenation of methyl (*Z*)- α -*N*-methyl-acetamidocinnamate to (*R*)-*N*-methyl-*N*-acetylphenylalanine methyl ester with **6a** (97% ee). Methyl (*Z*)- α -acetamidocinnamate is hydrogenated to (*R*)-*N*-acetylphenylalanine methyl ester with up to 96% ee with **6b** as the catalyst.

Introduction

Since the early introduction of DIPAMP in the pool of chiral ligands for enantioselective catalysis,¹ the development of diphosphines containing stereogenic P atoms has been hampered by the lack of amenable synthetic protocols fulfilling the requirements of large-scale preparations.² However, despite the apparent oblivion, several research groups have been developing procedures for the synthesis of enantiomerically pure *P*-chiral phosphines.^{3,4} These investigations have been paving the way for a number of recent applications of *P*-chiral diphosphines in enantioselective catalysis.⁵

Some of the new synthetic methods exploit the diastereoselective formation of a cyclic phospholidine intermediate³ (or related compounds)⁶ with a bifunctional chiral auxiliary, in which the configuration at the P atom is stabilized by a protecting group X. The latter can be BH₃,^{3a-c} oxide,^{3d} or sulfide.^{3e} Among these, the synthetic procedure for enantiomerically pure phosphine boranes, developed by Jugé (Scheme 1) starting from the pioneering work by Imamoto,⁷ offers several advantages in terms of chemical and configurational stability, ease of purification and deprotection, and extension to various substituents R.^{5f} A further advantage is that the intermediate phosphinite boranes P(Ph)(R)(OMe)-(BH₃) allow nucleophilic substitution at the P atom with retention of configuration.^{3g}

* To whom correspondence should be addressed. E-mail: mezzetti@inorg.chem.ethz.ch.

[†] X-ray structural studies of (*S,S*)-**2a** and **5a**.

[‡] For the synthesis and characterization of complex **5a**.

(1) Vineyard, B. D.; Knowles, W. S.; Sabacky, M. J.; Bachmann, G. L.; Weinkauff, D. J. *J. Chem. Am. Soc.* **1977**, *99*, 5946.

(2) (a) Pietrusiewicz, K. M.; Zablocka, M. *Chem. Rev.* **1994**, *94*, 1375. (b) Ohff, M.; Holz, J.; Quirnbach, M.; Börner, A. *Synthesis* **1998**, 1391.

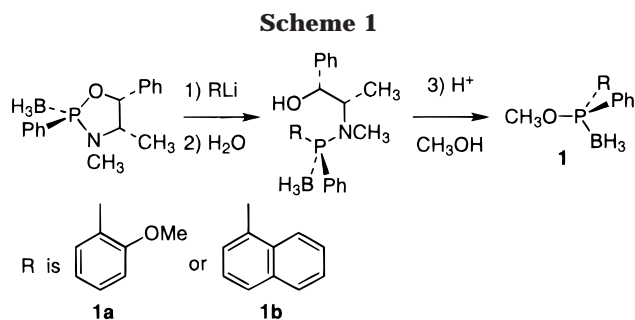
(3) (a) Jugé, S.; Stéphan, M.; Laffitte, J. A.; Genet, J. P. *Tetrahedron Lett.* **1990**, *31*, 6357. (b) Jugé, S.; Merdès, R.; Stéphan, M.; Genet, J. P. *Phosphorus, Sulfur, Silicon* **1993**, *77*, 199. (c) Jugé, S.; Stéphan, M.; Merdès, R.; Genet, J. P.; Halut-Desportes, D. *J. Chem. Soc., Chem. Commun.* **1993**, 531. (d) Carey, J. V.; Barker, M. D.; Brown, J. M.; Russell, M. J. H. *J. Chem. Soc., Perkin Trans. 1* **1993**, 831. (e) Corey, E. J.; Zhuoliang, C.; Tanoury, G. J. *J. Am. Chem. Soc.* **1993**, *115*, 11000. (f) Kaloun, E. B.; Merdès, R.; Genet, J. P.; Uziel, J.; Jugé, S. *J. Organomet. Chem.* **1997**, *529*, 455 (g) Brown, J. M.; Laing, J. C. P. *J. Organomet. Chem.* **1997**, *529*, 435. (h) Brunet, J.-J.; Chauvin, R.; Commenges, G.; Donnadiéu, B.; Leglaye, P. *Organometallics* **1996**, *15*, 1752. (i) Brodie, N.; Jugé, S. *Inorg. Chem.* **1998**, *37*, 2438.

(4) For methods based on enantioselective deprotonation, see: (a) Muci, A. R.; Campos, K. R.; Evans, D. A. *J. Am. Chem. Soc.* **1995**, *117*, 9075. (b) Wolfe, B.; Livinghouse, T. *J. Am. Chem. Soc.* **1998**, *120*, 5116.

(5) (a) Genêt, J. P.; Pinel, C.; Ratovelomanana-Vidal, V.; Mallart, S.; Pfister, X.; Caño De Andrade, M. C.; Laffitte, J. A. *Tetrahedron: Asymmetry* **1994**, *5*, 665. (b) Genêt, J. P.; Pinel, C.; Ratovelomanana-Vidal, V.; Mallart, S.; Pfister, X.; Bischoff, L.; Caño De Andrade, M. C.; Darses, S.; Galopin, C.; Laffitte, J. A. *Tetrahedron: Asymmetry* **1994**, *5*, 675. (c) Genêt, J. P.; Jugé, S.; Laffitte, J. A.; Pinel, C.; Mallart, S. (Elf Aquitaine), PCT Int. Appl. WO 01390, 1994 [*Chem. Abstr.* **1994**, *121*, P156763d]. (d) Zhu, G. X.; Terry, M.; Zhang, X. M. *Tetrahedron Lett.* **1996**, *37*, 4475. (e) Robin, F.; Mercier, F.; Ricard, L.; Mathey, F.; Spagnol, M. *Chem. Eur. J.* **1997**, *3*, 1365. (f) Stoop, R. M.; Mezzetti, A.; Spindler, F. *Organometallics* **1998**, *17*, 668. (g) Imamoto, T.; Watanabe, J.; Wada, Y.; Masuda, H.; Yamada, H.; Tsuruta, H.; Matsukawa, S.; Yamaguchi, K. *J. Am. Chem. Soc.* **1998**, *120*, 1635.

(6) Hersh, W. H.; Xu, P.; Simpson, C. K.; Wood, T.; Rheingold, A. L. *Inorg. Chem.* **1998**, *37*, 384.

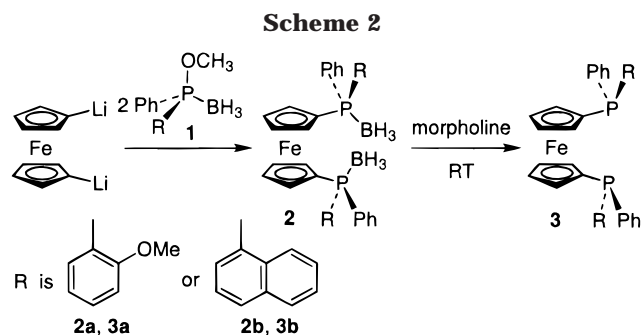
(7) Imamoto, T.; Oshiki, T.; Onozawa, T.; Kusumoto, T.; Kazuhiko, S. *J. Am. Chem. Soc.* **1990**, *112*, 5244.



Previous work from these laboratories showed that highly enantioselective asymmetric hydrogenation of dehydroamino acids is achieved with the ligand (*S,S*)-Me₂Si(CH₂P(1-Np)(Ph))₂ (1-Np = 1-naphthyl), based on a silane bridge.^{5f} However, as major drawbacks, this ligand could not be crystallized and is susceptible to cleavage at the silane bridge. These drawbacks suggested the use of the 1,1'-ferrocenediyl moiety as diphosphine bridge, since ferrocenyl phosphines are generally chemically stable, crystalline solids. As a further advantage, 1,1'-(diphosphino)ferrocenes exhibit large bite angles (typically about 100° for dppf complexes).⁸ Thus, we have been developing a general procedure for the introduction of two stereogenic P atoms into a 1,1'-ferrocenediyl moiety by nucleophilic substitution of 1,1'-dilithioferrocene onto the phosphinite boranes P(Ar)(Ph)(OMe)(BH₃), which extends a synthetic pathway recently devised by Brown for the synthesis of monodentate, *P*-chiral ferrocenyl phosphines.^{3g} The development of this approach allowed us to prepare the ligands (*S,S*)-1,1'-bis(2-methoxyphenyl(phenyl)phosphino)ferrocene (**3a**) and (*S,S*)-1,1'-bis(1-naphthyl(phenyl)phosphino)ferrocene (**3b**) in excellent enantiomeric purity and high to moderate yield. We report herein the full characterization of **3a,b** and their application in the enantioselective Rh-catalyzed hydrogenation of various substrates. Preliminary reports of the use of **3a,b** in asymmetric hydrogenation^{9a,d-f} and allylic alkylation^{9b,c} have appeared.

Results and Discussion

Synthesis of (*S,S*)-2a and (*S,S*)-2b. 1,1'-Dilithioferrocene reacts with (*R*)-2-methoxyphenyl(phenyl)-*O*-methylphosphinite borane^{3a} (**1a**) and (*R*)-1-naphthyl(phenyl)-*O*-methylphosphinite borane^{5f} (**1b**) giving (*S,S*)-1,1'-bis(2-methoxyphenyl(phenyl)phosphino)ferrocene borane (**2a**) and (*S,S*)-1,1'-bis(1-naphthyl(phenyl)phosphino)ferrocene borane (**2b**) (Scheme 2). The reaction of anisyl analogue **1a** is nearly quantitative. Partial loss of stereochemistry occurs, with the (*l*)- and (*u*)-diastereomers of **2a** formed in a 3.5:1 ratio. Column chromatography allows separation of (*l*)- and (*u*)-**2a**, which are



recovered from the reaction mixture in 72% and 20% chemical yield, respectively. As observed for analogous nucleophilic substitutions,^{3a-c} the reaction occurs with inversion of configuration at the P atom, as supported by an X-ray study of (*S,S*)-**2a** (see below). In the case of the naphthyl derivative (*R*)-**1b**, only (*l*)-**2b** is formed, albeit in lower chemical yield (48%). The free diphosphines **3a,b** are obtained by deboration of **2a,b** with morpholine at room temperature. Column chromatography yields analytically and enantiomerically pure (*S,S*)-**3a,b**.¹⁰

To ascertain the diastereomeric composition and the enantiomeric purity of the reaction products, we prepared a diastereomeric mixture of (*l*)- and (*u*)-**2a**. Treatment of 1,1'-dilithioferrocene with (*rac*)-**1a** (see Experimental Section) in 2:1 mole ratio gave both diastereomers of **2a**, which were isolated from the reaction mixture in an approximate (*l*):(*u*) ratio of 3:1. As the introduction of the second stereocenter occurs with significant diastereoselectivity, the epimerization observed in the reaction of (*S,S*)-**1a** apparently occurs in the first substitution step. The diastereomeric mixture was then separated by column chromatography into pure (*l*)-**2a** and (*u*)-**2a**. ¹H and ³¹P NMR spectroscopies, FAB⁺ MS, and elemental analysis support the chemical identity of the latter. Deboration as described above converts (*S,S*)+(*R,R*)-**2a** into (*S,S*)+(*R,R*)-**3a**.

Since low solubility precluded the use of HPLC on the chiral column, the enantiomeric purity of ligands (*S,S*)-**3a,b** was determined by ³¹P NMR spectroscopy on the corresponding phosphine oxides. The diphosphines (*S,S*)-**3a,b** were oxidized with H₂O₂ to (*R,R*)-1,1'-bis(*P*-oxo-2-methoxyphenyl(phenyl)phosphino)ferrocene, (*R,R*)-(**4a**) and (*R,R*)-1,1'-bis(*P*-oxo-1-naphthyl(phenyl)phosphino)ferrocene, (*R,R*)-(**4b**), respectively.¹² In the presence of the chiral solvating agent (*S*)-(+)-2,2,2-trifluoro-1-(9-anthryl)ethanol, (*R,R*)- and (*S,S*)-**4a,b** form diastereomeric adducts with resolved ³¹P NMR signals, whose integration shows that no more than 1% (*S,S*)-**4a,b** is present.¹³

X-ray Analysis of (*S,S*)-2a. Crystals of **2a** were grown from THF/hexane. An ORTEP drawing is shown

(8) Gan, K. S.; Hor, T. S. A. In *Ferrocenes*; Togni, A., Hayashi, T., Eds.; VCH: Weinheim, D, 1995.

(9) (a) Stoop, R. M.; Maienza, F.; Wong, T. Y. H.; Spindler, F. Mezzetti, A. OMCOS 9, Göttingen, Germany, 1997, abstract 291. (b) Nettekoven, U.; Kamer, P. C. J.; van Leeuwen, P. W. N. M. OMCOS 9, Göttingen, Germany, 1997; poster 300. (c) Nettekoven, U.; Widhalm, M.; Kamer, P. C. J.; van Leeuwen, P. W. N. M. *Tetrahedron: Asymmetry* **1997**, *8*, 3185. (d) Maienza, F.; Stoop, R. M.; Wong, T. Y. H.; Mezzetti, A. Assemblée d'automne de la Nouvelle Société Suisse de Chimie, Lausanne, Switzerland, 1997; poster 87. (e) Maienza, F. Laurea Thesis, Milan, Italy, May 1998. (f) Nettekoven, U.; Widhalm, M.; Kamer, P. C. J.; van Leeuwen, P. W. N. M. ISHC 11th, St. Andrews, Scotland, 1998; poster 28.

(10) The absolute configuration at the P atom is expressed in terms of the Cahn-Ingold-Prelog sequence rules¹¹ and, in the case of **3a,b**, refers to the uncoordinated ligand.

(11) Cahn, R. S.; Ingold, C. K.; Prelog, V. *Angew. Chem., Int. Ed. Engl.* **1966**, *5*, 385.

(12) (a) The oxidation at stereogenic P atoms is generally assumed to occur with retention of configuration at the P atom.^{12b} (b) Brown, J. M.; Carey, J. V.; Russell, M. J. H. *Tetrahedron* **1990**, *46*, 4877.

(13) In the case of **4a**, the signals were attributed by comparison with the ³¹P NMR spectrum of the racemic phosphine oxide (*R,R*)+(*S,S*)-**4a** recorded under the same conditions in the presence of excess (*S*)-(+)-2,2,2-trifluoro-1-(9-anthryl)ethanol, which shows two resolved singlets ($\Delta\nu = 8$ Hz).

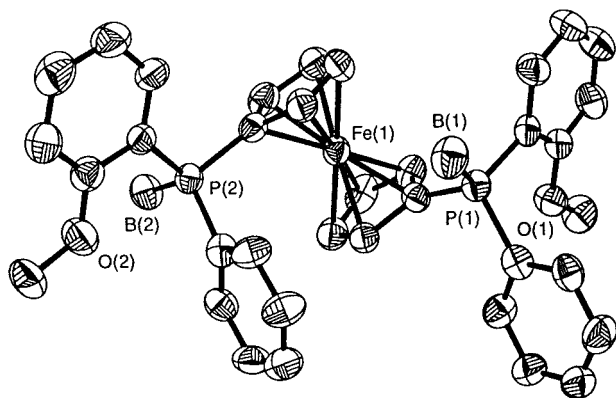


Figure 1. ORTEP view of (*S,S*)-1,1'-bis(2-methoxyphenyl)-(phenyl)phosphinoferrocene borane, **2a**.

Table 1. Selected Interatomic Distances (Å) and Angles (deg) in **2a**

P(1)–C(1)	1.794(5)	P(2)–C(19)	1.788(4)
P(1)–C(6)	1.808(4)	P(2)–C(24)	1.819(4)
P(1)–C(13)	1.819(4)	P(2)–C(31)	1.814(4)
P(1)–B(1)	1.940(6)	P(2)–B(2)	1.924(6)
C(1)–P(1)–C(6)	104.8(2)	C(19)–P(2)–C(24)	103.5(2)
C(1)–P(1)–C(13)	105.4(2)	C(19)–P(2)–C(31)	106.3(2)
C(1)–P(1)–B(1)	116.4(3)	C(19)–P(2)–B(2)	111.4(2)
C(6)–P(1)–C(13)	108.6(2)	C(24)–P(2)–B(2)	115.5(2)
C(6)–P(1)–B(1)	112.2(3)	C(24)–P(2)–C(31)	104.9(2)
C(13)–P(1)–B(1)	108.9(2)	C(31)–P(2)–B(2)	114.3(2)
C(11)–O(1)–C(12)	118.1(4)	C(29)–O(2)–C(30)	117.5(4)

in Figure 1, and selected bond distances and angles are reported in Table 1. The crystal contains discrete molecules of **2a** with normal nonbonded interactions. The distorted tetrahedral geometry of the P atom is typical of phosphine borane adducts.¹⁴ The conformation is anticlinal staggered:⁸ the P(1)–X(1)–X(19)–P(2) torsional angle τ is -116.2° (X are the centroids of the Cp rings). The Cp rings are parallel within 1° , and P(1) and P(2) are slightly pushed away from the Fe atom: the distances from the corresponding planes of the Cp rings are 0.019 and 0.026 Å, respectively. The (*S,S*)-configuration of the P atoms is supported by refinement of the Flack x parameter and is in agreement with inversion of configuration occurring at the P atom in the nucleophilic substitution step (Scheme 2).

[PtCl₂((*S,S*)-3a**)] (**5a**).** The platinum derivative [PtCl₂((*S,S*)-**3a**)] (**5a**) was prepared by reaction of [PtCl₂(PhCH=CH₂)₂] with (*S,S*)-**3a** in toluene. An X-ray study, whose results are summarized in Table 2 and Figure 2, discloses the details of the coordination mode of **3a**. The unit cell contains two crystallographically independent [PtCl₂((*S,S*)-**3a**)] units (molecules **5a'** and **5a''**), together with one CH₂Cl₂ molecule as solvent of crystallization. Least-squares refinement of the sign of $\Delta f''$ ($\eta = +1.0(2)$) supports the (*S,S*)-configuration, in agreement with the above assumption that deboration occurs with retention of configuration.

The overall geometry of the ligand **3a** is similar in both independent molecules and is analogous to that of dppf in square planar complexes of platinum(II),⁸ with bite angles of $102.0(1)^\circ$ and $99.6(1)^\circ$ in **5a'** and **5a''**,

respectively. The ferrocenyl moieties display synclinal (staggered) conformations: the P(1)–X(1)–X(19)–P(2) torsional angles τ in **5a'** and **5a''** are 39.7° and 34.0° (X represent the centroids of the Cp rings).⁸ The angle θ between the Cp planes is 5.4° (**5a'**) and 7.4° (**5a''**), with both P diverging from coplanarity with the Cp rings within ± 0.08 Å. However, the conformations of the two independent molecules are markedly different. Molecule **5a'** is pseudo-*C*₂ symmetric about the Pt–Fe vector, since both methoxy groups are oriented toward the metal. In the chelate ring, the phenyls are pseudoaxial, and the anisyl groups pseudoequatorial (Figure 3). The Fe atom lies very nearly in the Pt–Cl(1)–Cl(2)–P(1)–P(2) plane, the distance from best plane being 0.14 Å (Figure 2, **5a'**). The pseudo-*C*₂ symmetry is destroyed in **5a''**: one OMe group is rotated away from the Pt atom: the Pt(1')–P(2')–C(24')–C(29') torsion angle is $169.9(8)^\circ$. The torsional strain about the Pt–P(2) bond pushes the ferrocenyl moiety away from the plane of the complex (Figure 3): the distance between Fe and best plane is now 1.38 Å. No Pt...Fe interactions exist in either **5a'** or **5a''**.

In agreement with the X-ray data, molecular modeling (UFF calculations based on the Cerius² program)¹⁵ indicates that **5a'** and **5a''** have nearly the same total energy (1403.93 and 1405.48 kcal mol⁻¹, respectively). Thus, we have investigated the solution behavior of **5a** with respect to the interconversion of the conformers. The ¹H and ³¹P NMR of **5a** indicate that the 2-methoxyphenyl substituents freely rotate at room temperature: a single ¹H NMR signal is observed for the two equivalent methoxy groups, and the ³¹P NMR spectrum exhibits a sharp singlet with ¹⁹⁵Pt satellites. The low-temperature ¹H and ³¹P NMR spectra show that the anisyl rotation slows down upon cooling, since the ³¹P NMR signals broaden below -20°C ($w_{1/2}$ of the central signal is 81 Hz at -80°C). However, the barrier to rotation must be low, as the signals of the two conformers do not decoalesce down to -90°C . In the ¹H NMR spectra, the Cp and OMe signals broaden below -40°C , but decoalescence is not achieved at -90°C , the lowest available temperature.

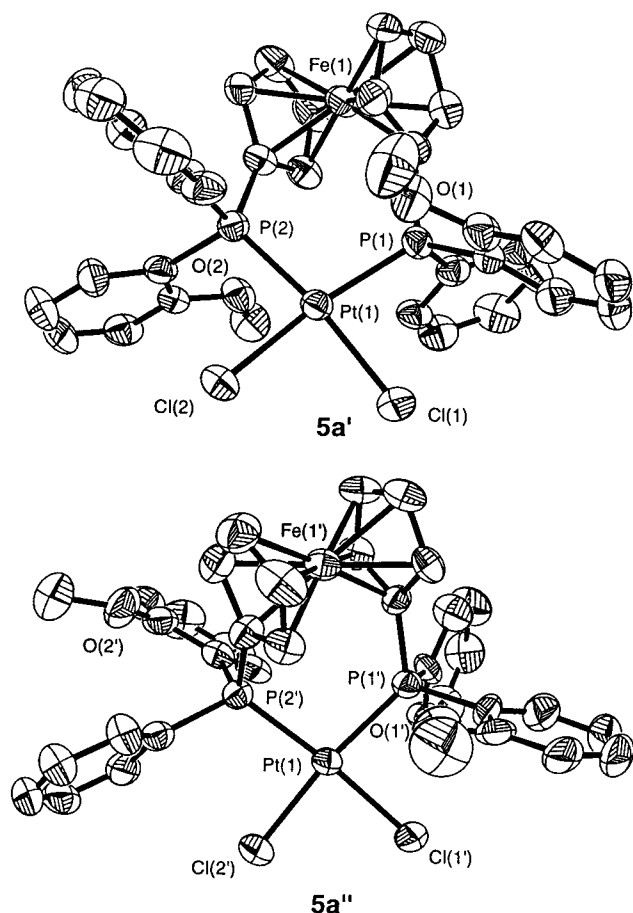
[Rh(COD)(3a,b**)]BF₄ (**6a,b**).** The rhodium derivatives [Rh(COD)(P–P*)]BF₄ (P–P* = (*S,S*)-**3a**, **6a**; P–P* = (*S,S*)-**3b**, **6b**) were prepared by reaction of the free ligands **3a,b** with [Rh(COD)₂]BF₄. The solution NMR spectra of **6a,b** indicate a dynamic behavior apparently related to the restricted rotational freedom of the *o*-anisyl or 1-naphthyl substituents. The room-temperature ³¹P NMR spectrum of **6a** consists of a broad doublet centered at δ 18.9 (CD₂Cl₂, 162 MHz, $w_{1/2} = 291$ Hz, $J_{\text{RhP}} = 144$ Hz). This signal coalesces at 0°C into a broad hump centered at δ 17.3 ($w_{1/2} \approx 340$ Hz), which resolves into a doublet upon further cooling. At -80°C , a sharp doublet at δ 17.08 ($J_{\text{RhP}} = 153$ Hz) is the only signal. The solution behavior of **6a,b** can be explained assuming the presence of two conformers with different populations, whereby the symmetric one **6'** predominates over the asymmetric conformer **6''**. At room temperature, the two conformers are interconverted on the NMR time scale, giving an unresolved, broad

(14) (a) Huffmann, J. C.; Skupinski, W. A.; Caulton, K. G. *Cryst. Struct. Commun.* **1982**, *11*, 1435. (b) Schmidbaur, H.; Wimmer, T.; Lachmann, J.; Müller, G. *Chem. Ber.* **1991**, *124*, 275. (c) Schmidbaur, H.; Stützer, A.; Bissinger, P.; Schier, A. *Z. Anorg. Allg. Chem.* **1993**, *619*, 1519.

(15) (a) Rappé, A. K.; Casewit, C. J.; Colwell, K. S.; Goddard, W. A., III; Skiff, W. M. *J. Am. Chem. Soc.* **1992**, *114*, 10024. (b) Rappé, A. K.; Colwell, K. S.; Casewit, C. J. *Inorg. Chem.* **1993**, *32*, 3438.

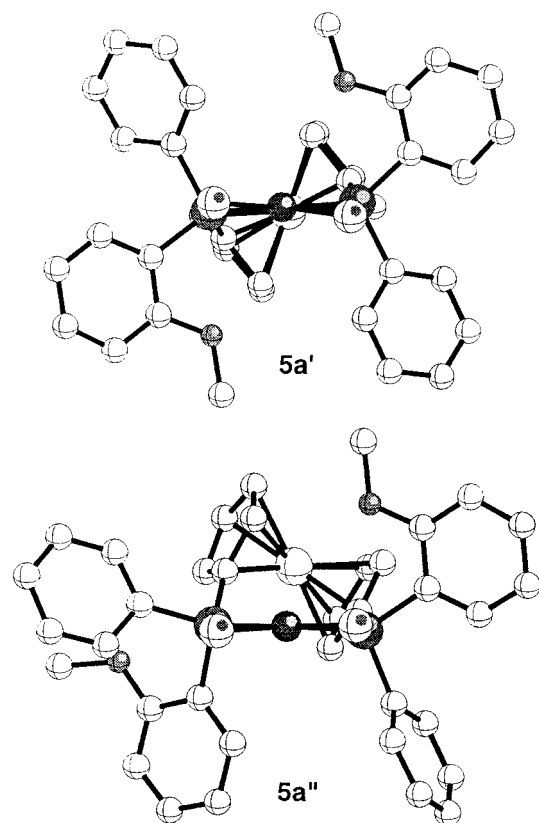
Table 2. Selected Interatomic Distances (Å) and Angles (deg) in **5a**

5a'		5a''	
Pt(1)–P(1)	2.254(3)	Pt(1')–P(1')	2.266(3)
Pt(1)–P(2)	2.254(3)	Pt(1')–P(2')	2.268(3)
Pt(1)–Cl(2)	2.342(3)	Pt(1')–Cl(2')	2.334(3)
Pt(1)–Cl(1)	2.353(3)	Pt(1')–Cl(1')	2.344(3)
Pt(1)⋯Fe(1)	4.288(2)	Pt(1')⋯Fe(1')	4.240(2)
P(1)⋯P(2)	3.504(4)	P(1')⋯P(2')	3.463(4)
<hr/>			
P(1)–Pt(1)–P(2)	102.0(1)	P(1')–Pt(1')–P(2')	99.6(1)
P(1)–Pt(1)–Cl(2)	169.6(1)	P(1')–Pt(1')–Cl(2')	170.1(1)
P(2)–Pt(1)–Cl(2)	87.0(1)	P(2')–Pt(1')–Cl(2')	89.1(1)
P(1)–Pt(1)–Cl(1)	84.4(1)	P(1')–Pt(1')–Cl(1')	85.6(1)
P(2)–Pt(1)–Cl(1)	170.0(1)	P(2')–Pt(1')–Cl(1')	174.8(1)
Cl(2)–Pt(1)–Cl(1)	87.4(1)	Cl(2')–Pt(1')–Cl(1')	85.9(1)
<hr/>			
Pt(1)–P(1)–C(6)–C(11)	–66.7(9)	Pt(1')–P(1')–C(6')–C(11')	–57(1)
Pt(1)–P(1)–C(13)–C(14)	8.7(9)	Pt(1')–P(1')–C(13')–C(14')	–33(1)
Pt(1)–P(2)–C(24)–C(29)	–68.6(9)	Pt(1')–P(2')–C(24')–C(29')	169.9(8)
Pt(1)–P(2)–C(31)–C(32)	0(1)	Pt(1')–P(2')–C(31')–C(32')	–77.5(9)

**Figure 2.** ORTEP view of **5a'** and **5a''**.

spectrum. Lowering the temperature below 0 °C not only slows down the exchange process but also shifts the conformer population toward the more stable symmetric species. Thus, at –80 °C only the latter is observed in the case of the anisyl derivative **6a**. Molecular modeling confirms this interpretation (Figure 4; see the Supporting Information for details): the C_2 -symmetric conformer **6a'** is more stable than the C_1 -symmetric **6a''** by ca. 6 kcal mol^{–1} (**6a'** 1719.95 kcal mol^{–1}, **6a''** 1726.17 kcal mol^{–1}).

In the case of **6b**, both conformers are observed at low temperature. The broad ³¹P NMR spectrum observed at room temperature (δ 19.3, $w_{1/2}$ = 360 Hz, CD₂Cl₂, 162 MHz) decoalesces between 20 and 0 °C to give, at

**Figure 3.** Ball and stick view of **5a'** and **5a''** along the P–Cl vectors (X-ray data).

–40 °C, a sharp doublet (δ 19.0, J_{RHP} = 151 Hz) for **6b'** and two slightly broadened doublets of doublets (δ_A 19.3, J_{RHP} = 153, $J_{\text{PP}'}$ = 17.8 Hz; δ_B 16.1, J_{RHP} = 147, $J_{\text{PP}'}$ = 17.8 Hz). Integration of these signals gives a **6b'**:**6b''** ratio of 54:46. In the ¹H NMR spectrum at –60 °C, the inequivalent naphthyl C² protons of the asymmetric conformer give rise to well-resolved signals at δ 10.1 and 10.7, whereas those of the symmetric one appear as a multiplet centered at δ 8.4.

Molecular modeling predicts, at least qualitatively, the different behavior of **6b** compared to **6a**, the energy gap being lower (ca. 5 kcal mol^{–1}; **6b'**, 1736.75 kcal mol^{–1}, **6b''** 1741.73 kcal mol^{–1}) than in **6a**. However, a quantitative correlation between the calculated total energy and the observed conformer distribution in the ³¹P NMR experiment cannot be expected, since the

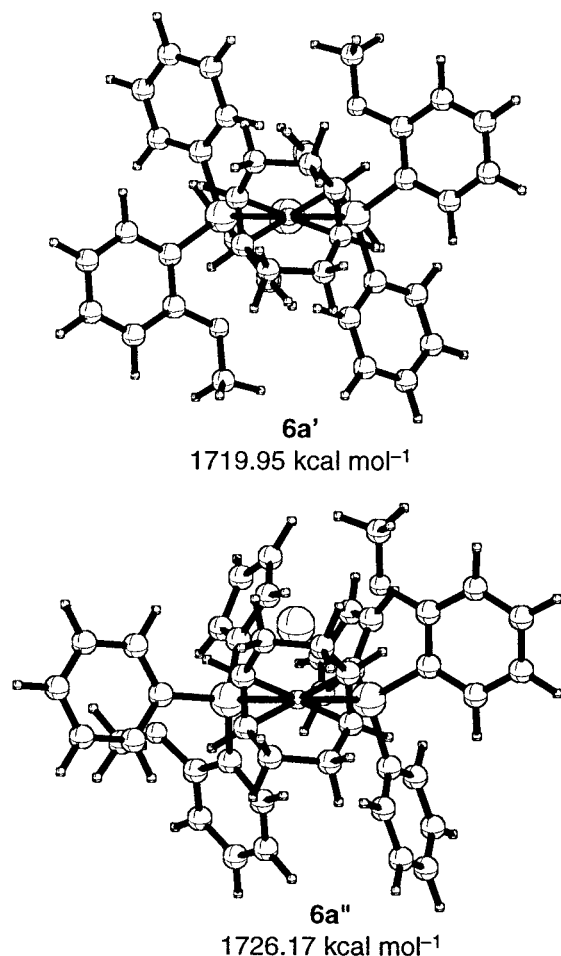
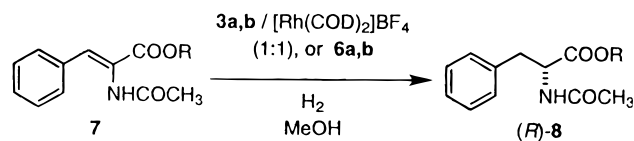


Figure 4. Conformers **6a'** (symmetric) and **6a''** (asymmetric) with minimized energies (Cerius² molecular modeling calculations).

barriers to rotation probably play a role in preventing the system reaching the thermal equilibrium as the sample temperature is lowered. Also, the absolute total energy values calculated for **6a** and **6b** indicate that the 1-naphthyl derivative **3b** is more bulky than its anisyl analogue **3a**.

Rhodium-Catalyzed Hydrogenation. Ligands **3a,b** were tested in the rhodium(I)-catalyzed hydrogenation of functionalized olefins and ketones. The results of the asymmetric hydrogenation of α -acetamidocinnamic acid derivatives are summarized in Tables 3 and 4. The isolated complex **6a** hydrogenates methyl (*Z*)- α -acetamidocinnamate (**7**) to (*R*)-*N*-acetylphenylalanine methyl ester (**8**) with 96% ee at 20 °C and 1 bar H₂ (Table 3, run 1). By contrast, the catalytic system formed in situ from **3a** and [Rh(COD)₂]BF₄ gives only 91% ee under identical reaction conditions (run 3). Since the enantiomeric purity of the ligands has been systematically checked, this significantly different enantioselectivity is possibly due to partial epimerization of the uncoordinated ligand under reaction conditions before the complex is formed. Increasing the temperature or the initial H₂ pressure decreases the enantioselectivity (runs 2, 4, 5). (*Z*)- α -Acetamidocinnamic acid is hydrogenated to (*R*)-*N*-acetylphenylalanine with the same enantioselectivity (run 6) as the methyl ester under the same conditions (run 4). The hydrogenation of **7** is catalyzed by complex **6b** with good enantioselectivity (92%, run

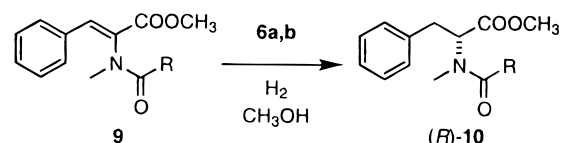
Table 3. Asymmetric Hydrogenation of **7** to **8**^a



run	catalyst	R	$p(\text{H}_2)$ (bar)	T (°C)	ee (%)
1	6a	Me	1	20	96
2	6a	Me	5	20	94
3	3a ^b	Me	1	20	91
4	3a ^b	Me	1	35	88
5	3a ^b	Me	20	35	85
6	3a ^{b,c}	H	1	35	88
7	6b	Me	1	20	92

^a Reaction conditions: MeOH (10 mL) as solvent, S/C = 200 (unless otherwise stated), reaction time 15–20 h, conversion 95–99.5%. ^b Catalyst formed in situ from **3a** (18 μ mol) and [Rh-(NBD)₂]BF₄ (6.4 mg, 17 μ mol), 3/Rh = 1.05. ^c S/C = 100, NEt₃ (9.5 μ L) added to the reaction solution.

Table 4. Asymmetric Hydrogenation of **9** to **10**^a



run	catalyst	R	$p(\text{H}_2)$ (bar)	ee (%)
1	6a	Me	1	97
2	6a	Me	5	97
3	6a	Ph	5	93
4	6b	Me	1	90
5	6b	Me	5	83

^a Reaction conditions: MeOH (10 mL) as solvent, S/C = 200, T = 25 °C, reaction time 17 h, conversion 99%.

7), but significantly lower than that obtained with the closely related precatalyst [Rh(COD)((*S,S*)-Me₂Si(CH₂P(1-Np)(Ph))₂)]⁺ (98% ee).^{5f}

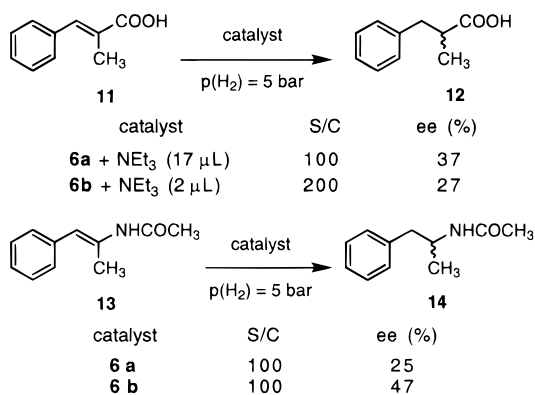
Ligands **3a,b** exhibit superior efficiency and enantio-discrimination in the asymmetric hydrogenation of *N*-substituted acetamidocinnamates, a class of substrates that is hydrogenated slowly and with much lower ee's than the unsubstituted analogues by most rhodium-based systems.^{1,16,17} Thus, **6a** quantitatively hydrogenates methyl (*Z*)- α -*N*-methyl-acetamidocinnamate (**9**) to (*R*)-*N*-methyl-*N*-acetylphenylalanine methyl ester (**10**) with 97% ee (Table 4, run 1). This value, which is slightly higher than that obtained with [Rh(COD)((*S,S*)-Me₂Si(CH₂P(1-Np)(Ph))₂)]BF₄,^{5f} is the best ever observed for *N*-substituted enamides. It should be also noted that recent reports of the hydrogenation of dehydroamino acids,¹⁸ even with *P*-chiral diphosphines,^{5g} do not encompass applications to *N*-substituted enamides. Introducing a benzamido group is detrimental to the enantioselectivity (run 3). With catalyst **6b**, **10** is obtained with lower enantioselectivity (90%, run 4) than with **6a**, confirming the trend observed with acetamidocinnamic acid **7**.

(16) Glaser, R.; Geresh, S.; Twai, M.; Benoiton, N. L. *Tetrahedron* **1978**, *34*, 3617.

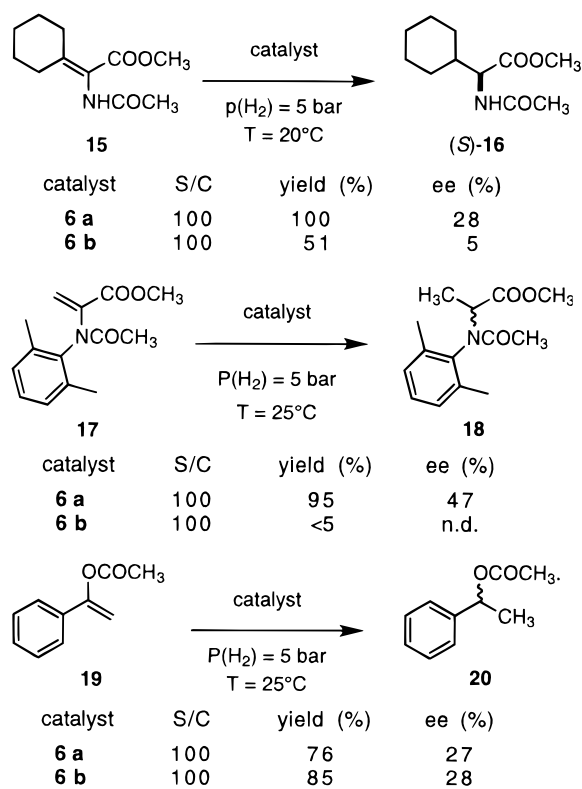
(17) Buser, H. P.; Pugin, B.; Spindler, F.; Sutter, M. *Tetrahedron* **1991**, *47*, 5709.

(18) (a) Pye, P. J.; Rossen, K.; Reamer, R. A.; Tsou, N. N.; Volante, R. P.; Reider, P. J. *J. Am. Chem. Soc.* **1997**, *119*, 6207. (b) Zhu, G.; Cao, P.; Jiang, Q.; Zhang, X. *J. Am. Chem. Soc.* **1997**, *119*, 1799.

Scheme 3



Scheme 4



Reaction conditions: methanol (10 mL) as solvent, reaction time 16–18 h.

The directing effect of the acylamino and the ester groups has been investigated. Both directing groups are necessary for high enantioselection. Thus, when the amido group is substituted with methyl, as in (*E*)-1-methylcinnamic acid (**11**), the ee values of the hydrogenation product (*E*)-1-methylhydrocinnamic acid (**12**) drop to 37–27% (Scheme 3). Also, (*E*)-2-acetamido-1-phenylpropene (**13**) is hydrogenated to 2-acetamido-1-phenylpropane (**14**) with low enantioselectivity (25–47%). Also the substitution pattern at enamide β-C atom plays a major role for enantioselection (Scheme 4). Thus, **6a** hydrogenates a β-disubstituted substrate such as acetylamino(cyclohexylidene)acetic acid methyl ester (**15**) to (*S*)-2-cyclohexylglycine methyl ester (**16**) with only 28% ee, whereas **6b** gives nearly racemic product. Interestingly, in both cases the sign of the enantioselection is reversed as compared to (*R*)-*N*-acetyl-

Table 5. Asymmetric Hydrogenation of Ketones^a

run	ligand	substrate	S/C	ee (%)
1	3a	21	100	26
2	3a	22	100	11
3	3a	23	100	29
4	3b	22	200	34

^a Reaction conditions: catalyst formed in situ from **3a,b** and [RhCl(NBD)]₂ (2:1 mol ratio); toluene (10 mL) as solvent, *p*(H₂) = 40 bar, *T* = 25 °C, reaction time 16–72 h, conversion 82–99%.

phenylalanine methyl ester (**8**). This fact, together with the low activity observed for **6b** in the hydrogenation of **15**, indicates that the catalytic system is highly sensitive to steric factors. As for β-unsaturated substrates, methyl 2-(*N*-2,6-dimethylphenyl-acetyl)aminoacrylate (**17**) gives the corresponding alanine derivative (**18**) in 47% ee with **6a** as the catalyst, whereas **6b** is nearly inactive. Finally, 1-phenylvinyl acetate (**19**) gives 1-phenylethyl acetate (**20**) with low enantioselectivity (27–28%). Taken together, these results suggest that the scope of ligands **3a,b** in the rhodium-catalyzed asymmetric hydrogenation of functionalized olefins is narrower than in the case of Imamoto's ligands (R)(Me)-PCH₂CH₂P(R)(Me)^{5g} or DUPHOS.¹⁹

The in situ catalytic system **3a,b**/[RhCl(COD)] hydrogenates ketones with low to moderate enantioselectivity (Table 5). Phenylglyoxylic acid methyl ester (**21**), ethyl pyruvate (**22**), and keto pantolactone (**23**) give methyl mandelate, ethyl lactate, and pantolactone with ee's between 34 and 11%. These values further indicate that the scope of ligands **3a,b** is essentially restricted to functionalized acetamido cinnamates, at least in the rhodium-catalyzed asymmetric hydrogenation.

Concluding Remarks. The rhodium(I) derivatives of **3a,b** are excellent catalysts for the asymmetric hydrogenation of acetamidocinnamates with high enantioselectivities, in particular *N*-alkylated derivatives. This gives access to *N*-alkylated amino acids, a class of compounds that are potentially interesting intermediates for pharmaceuticals. Also, ligands **3a,b** are among the first examples of a class of diphosphines bearing stereogenic P atoms in connection with large bite angles (≈100°). The comparison with the previously reported ligand (*S,S*)-Me₂Si(CH₂P(1-Np)(Ph))₂ (bite angle ≈ 93° according to molecular modeling) shows that the size of the bite angle does not improve ipso facto the catalytic performance in the rhodium-catalyzed hydrogenation of dehydroamino acids. In fact, our X-ray and NMR investigations on the Pt(II) and Rh(I) derivatives **5** and **6** show that different conformations are simultaneously present both in solution and in the solid state. This is apparently due to the torsional flexibility of the 1,1'-ferrocenediyl bridge and to the rotational freedom about the P–C bond of the aryl substituents at the P atoms. We are currently trying to enhance the rigidity of the ligand backbone with the aim of improving the enantio-

(19) See, for instance: Burk, M. J.; Gross, M. F.; Martinez, J. P. *J. Am. Chem. Soc.* **1995**, *117*, 9375.

selectivity of the catalytic hydrogenation of a larger scope of substrates.

Experimental Section

General Comments. Reactions with air- or moisture-sensitive materials were carried out under an argon atmosphere using Schlenk techniques. Solvents were purified according to standard procedures; (*R*)-**1a**,^{3a} (*R*)-**1b**,^{5f} and [PtCl₂-(η^2 -styrene)₂]²⁰ were prepared by published procedures. NMR spectra were recorded on Bruker DPX 250 or, when specified, 400 spectrometers. ¹H and ³¹P positive chemical shifts in ppm are downfield from tetramethylsilane and external 85% H₃PO₄, respectively. The ¹H and ³¹P NMR spectra of the P-BH₃ borane adducts **2a**, **b** are partially relaxed, nonbinomial 1:1:1 quartets due to coupling to ¹¹B (80.1% natural abundance); ¹J_{BH} and ¹J_{PB} were measured between the central peaks. Mass spectra were measured by the MS service of the Laboratorium für Organische Chemie (ETH Zürich). A 3-NOBA (3-nitrobenzyl alcohol) matrix and a Xe atom beam with a translational energy of 8 keV were used for FAB⁺ MS. HPLC was performed on a Hewlett-Packard 1050 chromatograph equipped with a variable wavelength detector and Daicel Chiralcel OD-H or OB-H columns (0.46 cm × 25 cm). Optical rotations were measured using a Perkin-Elmer 341 polarimeter with a 1 dm cell. Elemental analyses were carried out by the Laboratory of Microelemental Analysis (ETH Zürich). Melting points were measured in open capillaries with a Büchi-510 apparatus and are uncorrected.

(*S,S*)-1,1'-Bis(2-methoxyphenyl(phenyl)phosphino)ferrocene Borane, (*S,S*)-2a**.** 1,1'-Dilithioferrocene is prepared by addition of BuLi (25.7 mL, 0.0404 mol, 1.57 M in hexane) and TMEDA (4.69 g, 0.0404 mol, d 0.775 g/mL, 6.0 mL) to a hexane solution (150 mL) of ferrocene (3.76 g, 0.0202 mol) at room temperature. The orange precipitate formed upon stirring for 4 h is filtered off and dissolved in THF (150 mL). A THF solution (50 mL) of (*R*)-**1a** (10.51 g, 0.0404 mol) is added thereto dropwise. After stirring the resulting dark red solution for 2 h, the reaction is quenched with H₂O (50 mL). The product is extracted with *t*-BuOMe, and the combined organic layers are washed twice with a CuSO₄ solution and then with a NH₄Cl solution and dried with MgSO₄. Evaporation of the solvent and flash chromatography (silica gel, hexane/AcOEt (4:1)) gives analytically pure (*S,S*)-**2a** (*R*_f 0.12) and (*R,S*)-**2a** (*R*_f 0.19) as orange crystalline solids. (*S,S*)-**2a**: Yield: 9.27 g (72%); mp 168 °C. [α]_D²⁰ = -60.5° (CHCl₃, *c* = 1). ³¹P NMR (CDCl₃): δ 12.9 (br *q*, 2P). ¹H NMR (CDCl₃): δ 7.70–7.61 (m, 2H, *H*^b *o*-An), 7.49–7.26 (m, 12H, 2 C₆H₅, *H*^d *o*-An), 7.03–6.99 (m, 2H, *H*^e *o*-An), 6.86–6.81 (m, 2H, *H*^f *o*-An), 4.43–4.33 (m, 8H, 2 CpH), 3.42 (s, 6H, 2 OCH₃), 1.56–0.66 (m, 6H, 2 BH₃). MS (FAB⁺): *m/z* 642 (M⁺, 1), 628 (M⁺ - BH₃, 5), 614 (M⁺ - 2 BH₃, 100). Anal. Calcd for C₃₆H₃₈B₂FeO₂P₂: C, 67.34; H, 5.96. Found: C, 67.14; H, 6.21. (*R,S*)-**2a**: Yield: 2.67 g (21%). ³¹P NMR (CDCl₃): δ 13.0 (br *q*, 2P). ¹H NMR (CDCl₃): δ 7.92–7.83 (m, 2H, *H*^b *o*-An), 7.54–7.18 (m, 12H, 2 C₆H₅, *H*^d *o*-An), 7.11–6.99 (m, 2H, *H*^e *o*-An), 6.89–6.85 (m, 2H, *H*^f *o*-An), 4.57–4.15 (m, 8H, 2 CpH), 3.44 (s, 6H, 2 OCH₃), 1.56–0.66 (m, 6H, 2 BH₃). MS (FAB⁺): *m/z* 641 (M⁺, 49), 628 (M⁺ - BH₃, 39), 614 (M⁺ - 2 BH₃, 100), 507 (M⁺ - 2 BH₃ - *o*-An, 6). Anal. Calcd for C₃₆H₃₈B₂FeO₂P₂: C, 67.34; H, 5.96. Found: C, 67.53; H, 6.16.

X-ray Analysis of (*S,S*)-2a**.** Orange crystals of (*S,S*)-**2a** suitable for X-ray analysis were grown from THF/hexane (1:3). A prism (0.48 × 0.30 × 0.27 mm) was mounted on a glass capillary. Crystal data for C₃₆H₃₈B₂FeO₂P₂ (fw 614.43): triclinic, space group *P*₁, cell dimensions (298 K) *a* = 7.8770(10) Å, *b* = 8.7930(10) Å, *c* = 13.087(2) Å, α = 93.309(13)°, β = 105.005(12)°, γ = 108.641(12)°, and *V* = 819.77(19) Å³ with *Z* = 1 and *D*_c = 1.301 Mg/m³, μ = 0.589 mm⁻¹ (Mo K α , graphite

monochromated), λ = 0.71073 Å, *F*(000) = 336. The data were collected at room temperature on a STOE IPDS (image plate detector system) in the θ range 4.13–24.22°. Unit cell dimensions determination, data reduction, and absorption correction were performed with the STOE program package. The structure was solved with SHELXS-96 using direct methods.²¹ Of the 9431 measured reflections with index ranges $-9 \leq h \leq 9$, $-10 \leq k \leq 10$, $-15 \leq l \leq 15$, 4872 independent reflections (*R*_{int} = 0.0630) were used in the refinement, 414 parameters, full-matrix least-squares on *F*², quantity minimized $\sum w(|F_o|^2 - |F_c|^2)^2$ ($w^{-1} = \sigma^2(F_o^2) + (0.0155P)^2 + 0.51P$, where $3P = \max(F_o^2, 0) + 2F_c^2$) with anisotropic displacement parameters for all non-H atoms. Hydrogen atoms were introduced at calculated positions and refined with the riding model and individual isotropic thermal parameters for each group. The H atoms on B(1) and B(2) were fully refined. The absolute configuration at the P atoms was determined to be (*S,S*) by refinement of the Flack *x* parameter = -0.014(17). Final residuals (*I* > 2 σ (*I*)) were *R*₁ = 0.0372 and *wR*₂ = 0.0863 (all data *R*₁ = 0.0428 and *wR*₂ = 0.0920), GOF 1.065. Max. and min. difference peaks were +0.26 and -0.25 eÅ⁻³; largest and mean Δ/σ = 0.008 and 0.001. Molecular graphics were performed with the program XP with 50% ellipsoids. Atomic coordinates, anisotropic displacement coefficients, and an extended list of interatomic distances and angles are available as Supporting Information. Selected interatomic distances and angles are reported in Table 1.

(*S,S*)-1,1'-Bis(1-naphthyl(phenyl)phosphino)ferrocene Borane, (*S,S*)-2b**.** An Et₂O solution (21 mL) of **1b** (1.50 g, 5.36 mmol) is added dropwise to a THF solution (8 mL) of 1,1'-dilithioferrocene (2.7 mmol), prepared as described above. After stirring the dark red solution for 2 h, the reaction is quenched with H₂O (10 mL). Workup is as for **2a**. Flash chromatography (silica gel, hexane/AcOEt (9:1)) gives analytically pure (*S,S*)-**2b** (*R*_f 0.15) as an orange crystalline solid. Yield: 0.88 g (48%); mp 163 °C. [α]_D²⁰ = +45.8° (CHCl₃, *c* = 1). ³¹P NMR (CDCl₃): δ 16.2 (br, 2P). ¹H NMR (CDCl₃): δ 7.95–7.77, 7.59–7.21 (2 m, 24H, ArH), 4.67 (s, 4H, 2 CpH), 4.57, 3.83 (2 s, 4H, 2 CpH), 1.56–0.86 (m, 6H, 2 BH₃). MS (FAB⁺): *m/z* 681.1 (M⁺, 30), 668.1 (M⁺ - BH₃, 25), 654.0 (M⁺ - 2 BH₃, 100), 577.0 (M⁺ - 2 BH₃ - Ph, 4). Anal. Calcd for C₄₂H₃₈B₂FeP₂: C, 73.95; H, 5.61. Found: C, 73.93; H, 5.69.

(*S,S*)-1,1'-Bis(2-methoxyphenyl(phenyl)phosphino)ferrocene, (*S,S*)-3a**.** Compound (*S,S*)-**2a** (9.270 g, 14.4 mmol) is dissolved in morpholine (30 mL), and the solution is stirred overnight at room temperature, evaporated to dryness (at room temperature), and purified by flash chromatography (silica gel, hexane/AcOEt (4:1), *R*_f 0.4). Yield: 7.62 g (86%); mp 152 °C. [α]_D²⁰ = +176.1° (CHCl₃, *c* = 1). ³¹P NMR (CDCl₃): δ -30.1 (s, 2P). ¹H NMR (CDCl₃): δ 7.37–6.77 (2 m, 18H, 2 C₆H₅, 2 *o*-An), 4.41, 4.40, 4.39, 3.58 (4 s, 8H, 2 CpH), 3.67 (s, 6H, 2 OCH₃). MS (FAB⁺): *m/z* 614.1 (M⁺, 100), 537.1 (M⁺ - Ph, 4), 507.0 (M⁺ - Ph - *o*-An, 4). Anal. Calcd for C₃₆H₃₂FeO₂P₂: C, 70.37; H, 5.25. Found: C, 70.12; H, 5.21.

(*S,S*)-1,1'-Bis(1-naphthyl(phenyl)phosphino)ferrocene, (*S,S*)-3b**.** Compound (*S,S*)-**2b** (0.548 g, 0.803 mmol) is dissolved in morpholine (30 mL), and the solution is stirred 24 h at room temperature and then evaporated to dryness (at room temperature). Flash chromatography (silica gel, hexane/AcOEt (4:1), *R*_f 0.4) yields (*S,S*)-**3b**, which is recrystallized from hexane. Yield: 400 mg (76%); mp 153 °C. [α]_D²⁰ = +157.7° (CHCl₃, *c* = 1). ³¹P NMR (CDCl₃): δ -26.7 (s, 2P). ¹H NMR (CDCl₃): δ 8.37–8.32 (m, 2H, ArH), 7.82–7.68 (m, 4H, ArH), 7.46–7.11 (m, 18H, ArH), 4.38, 4.34, 4.26, 3.69 (4 s, 8H, 2 CpH). MS (FAB⁺): *m/z* 654.1 (M⁺, 100), 577.1 (M⁺ - Ph, 4). Anal. Calcd for C₄₂H₃₂FeP₂: C, 77.07; H, 4.93. Found: C, 77.20; H, 5.00.

(*R,R*)-1,1'-Bis(*P*-oxo-2-methoxyphenyl(phenyl)phosphino)ferrocene, (*R,R*)-4a**.** H₂O₂ (30%, 2 mL) is added to a

(20) Caseri, W. R.; Pregosin, P. S. *Organometallics* **1988**, *7*, 1373.

(21) SHELXTL Program Package V. 5.1; Bruker AXS, Madison, WI, 1997.

THF solution (5 mL) of **3a** (50 mg, 0.078 mmol). After stirring for 15 min, H₂O (10 mL) is added, the THF is evaporated, and the product is extracted with CH₂Cl₂. Evaporation of the solvent gives an orange oil. Yield: 52 mg (99%). ³¹P NMR (CDCl₃): δ 26.7 (s, 2P). After addition of (S)-(+)-2,2,2-trifluoro-1-(9-anthryl)ethanol (3 equiv vs **4a**): ³¹P NMR (CDCl₃): (R,R)-**4a**, δ 30.04 (s, 2P, >99%); (S,S)-**4a**, δ 30.12 (s, 2P, <1%); >98% ee.

(R,R)+(S,S)-1,1'-Bis(P-oxo-2-methoxyphenyl(phenyl)phosphino)ferrocene, (R,R)-4a. Racemic (*l*)-**4a** is similarly prepared from (*l*)-**3a**. ³¹P NMR (CDCl₃): δ 26.7 (s, 2P). After addition of (S)-(+)-2,2,2-trifluoro-1-(9-anthryl)ethanol (3 equiv vs **4a**): ³¹P NMR (CDCl₃): (S,S)-**4a**, δ 29.61 (s, 2P, 50%); (R,R)-**4a**, δ 29.69 (s, 2P, 50%).

(R,R)-1,1'-Bis(P-oxo-1-naphthyl(phenyl)phosphino)ferrocene, (R,R)-4b. The compound is prepared as described for **4a** from **3b**. ³¹P NMR (CDCl₃): δ 31.4 (s, 2P). After addition of (S)-(+)-2,2,2-trifluoro-1-(9-anthryl)ethanol (3 equiv vs **4b**): ³¹P NMR (CDCl₃): (R,R)-**4b**, δ 32.60 (s, 2P, >99%); (S,S)-**4b**, δ 32.68 (s, 2P, <1%); >98% ee.

(rac)-N,N-Diethylamino(2-methoxyphenyl)phenylphosphine. A solution of 2-methoxyphenyllithium (prepared adding BuLi (15.1 mL, 30 mmol, 1.98 M in hexane) to a THF solution (5 mL) of 2-bromoanisole (5.611 g, 30 mmol, *d* 1.502 g/mL, 3.8 mL) at -78 °C and stirring for 30 min) is slowly added by cannula to a THF solution (45 mL) of (rac)-P(NEt₂)(Ph)Cl (6.041 g, 30 mmol) precooled at -78 °C. The reaction solution is slowly warmed to room temperature and then quenched with H₂O (5 mL). After evaporation of THF under vacuum, the reaction crude is extracted with CH₂Cl₂, dried over MgSO₄, and distilled. Yield: 7.667 g (89%). ³¹P NMR (CDCl₃): δ 51.5 (s, P). ¹H NMR (CDCl₃): δ 8.15–7.23 (m, 9H, ArH), 3.27–3.13 (m, 4H, P–N(CH₂CH₃)₂), 0.94 (t, 6H, P–N(CH₂CH₃)₂, ³J_{HH'} = 7.1 Hz).

(rac)-2-Methoxyphenyl(phenyl)-O-methylphosphinite Borane, (rac)-1a. (rac)-P(NEt₂)(*o*-An)(Ph) (7.667 g, 26.7 mmol) is dissolved in a MeOH solution (50 mL) of H₂SO₄ (1 mL, 97%). After stirring 15 h at room temperature, the solvent is evaporated and the residue is dissolved in toluene (20 mL). BH₃·SMe₂ (2.037 g, 26.7 mmol, *d* 0.801 g/mL, 2.5 mL) is added, and the solution is stirred 2 h at room temperature. Evaporation of the solvent under vacuum yields a yellow oil, which is purified by column chromatography (silica gel, hexane/AcOEt (4:1), *R_f* 0.5). Yield: 4.25 g (61%). Same NMR data as for (R)-2-methoxyphenyl(phenyl)-O-methylphosphinite borane.^{3a}

(l)+(u)-1,1'-Bis(2-methoxyphenyl(phenyl)phosphino)ferrocene Borane, (l)+(u)-2a. A THF solution (10 mL) of (rac)-**1a** (3.430 g, 13.2 mmol) is added dropwise to a hexane solution of 1,1'-dilithioferrocene (prepared adding BuLi (8.9 mL, 13.2 mmol, 1.48 M in hexane) and TMEDA (1.227 g, 13.2 mmol, *d* 0.775 g/mL, 2.0 mL) to ferrocene (1.521 g, 6.6 mmol) dissolved in hexane (40 mL) and stirring for 4 h). Flash chromatography as for (S,S)-**2a**. (R,S)-**2a**: Yield: 381 mg (9%). ³¹P NMR (CDCl₃): δ 13.0 (br q, 2P). ¹H NMR (CDCl₃): δ 7.92–7.83 (m, 2H, H^β *o*-An), 7.54–7.18 (m, 12H, 2 C₆H₅, H^α *o*-An), 7.11–6.99 (m, 2H, H^β *o*-An), 6.89–6.85 (m, 2H, H^β *o*-An), 4.57–4.15 (m, 8H, 2 CpH), 3.44 (s, 6H, 2 OCH₃), 1.56–0.66 (m, 6H, 2 BH₃). (R,R+S,S)-**2a**: Yield: 1.338 g (32%). ³¹P NMR (CDCl₃): δ 12.9 (br q, 2P). ¹H NMR (CDCl₃): δ 7.70–7.61 (m, 2H, H^β *o*-An), 7.49–7.26 (m, 12H, 2 C₆H₅, H^α *o*-An), 7.03–6.99 (m, 2H, H^β *o*-An), 6.86–6.81 (m, 2H, H^β *o*-An), 4.43–4.33 (m, 8H, 2 CpH), 3.42 (s, 6H, 2 OCH₃), 1.56–0.66 (m, 6H, 2 BH₃). A third reaction product (*R_f* 0.37) is identified as ferrocenyl-2-methoxyphenylphosphine borane.^{3b} Yield: 332 mg (12%); mp 172 °C. ³¹P NMR (CDCl₃): δ 13.6 (br d, P, ¹J_{BP} = 68 Hz). ¹H NMR (CDCl₃): δ 7.83–7.74 (m, 1H, ArH), 7.57–7.27 (m, 6H, ArH), 7.10–7.03 (m, 1H, ArH), 6.90–6.86 (m, 1H, ArH), 4.68 (s, 1H, P–C₅H₄), 4.53 (s, 1H, P–C₅H₄), 4.49 (s, 2H, P–C₅H₄), 4.03 (s, 5H, CpH), 3.47 (s, 3H, OCH₃), 1.54–0.89 (m, 3H, BH₃). MS (FAB⁺): *m/z* 414.2 (M⁺, 55), 400.1 (M⁺ – BH₃,

100), 335.1 (M⁺ – Ph, 9), 323.1 (M⁺ – BH₃ – Ph, 12), 307.1 (M⁺ – *o*-An, 49).

(l)-3a. Deboronation and purification as described for (S,S)-**2a**. Yield: 86%; mp 152 °C. ³¹P NMR (CDCl₃): δ -30.1 (s, 2P). ¹H NMR (CDCl₃): δ 7.37–6.77 (2m, 18H, 2 C₆H₅, 2 *o*-An), 4.41, 4.40, 4.39, 3.58 (4 s, 8H, 2 CpH), 3.67 (s, 6H, 2 OCH₃).

(u)-3a. Compound (*u*)-**2a** (100 mg, 0.156 mmol) is dissolved in morpholine (5 mL), and the solution is stirred overnight at room temperature, evaporated to dryness (at room temperature), and purified by flash chromatography (silica gel, hexane/AcOEt (4:1), *R_f* 0.4). Yield: 78 mg (82%); mp 155 °C. ³¹P NMR (CDCl₃): δ -30.4 (s, 2P). ¹H NMR (CDCl₃): δ 7.40–7.24 (m, 12H, ArH), 6.88–6.77 (m, 6H, ArH), 4.41, 4.30, 4.25, 3.59 (4 s, 8H, 2 CpH), 3.69 (s, 6H, 2 OCH₃). MS (FAB⁺): *m/z* 614.1 (M⁺, 100), 537.1 (M⁺ – Ph, 4), 507.1 (M⁺ – Ph – *o*-An, 5). Anal. Calcd for C₃₆H₃₂FeO₂P₂: C, 70.37; H, 5.25. Found: C, 70.37; H, 5.37.

[PtCl₂((S,S)-3a)] (5a). A toluene solution (5 mL) of (S,S)-**3a** (77 mg, 0.126 mmol) is slowly added to a suspension of [PtCl₂(PhCH=CH₂)₂] (60 mg, 0.126 mmol) in toluene (20 mL). The resulting solution is then stirred at room temperature for 8 h. After removing the solvent under vacuum, the resulting powder is washed twice with pentane (3 mL). Column chromatography (silica gel, CH₂Cl₂/MeOH (5:1)) gives the pure product. Yield: 92%. ¹H NMR (300 MHz, CDCl₃): δ 3.68 (s, 6H, OCH₃), 4.27 (m, 2H, CpH), 4.36 (m, 2H, CpH), 4.43 (m, 4H, CpH), 6.75 (t × d, 2H, AnH), 6.93 (d × d, 2H, AnH), 7.76 (m, 8H, ArH), 7.81 (m, 2H, ArH), 7.92 (m, 4H, ArH). ³¹P NMR (CD₂Cl₂, 162 MHz): δ 10.17 (s+Pt-satellites, ¹J_{PtP} = 3901 Hz). Anal. Calcd for C₃₆H₃₂O₂P₂Cl₂FePt·0.25CH₂Cl₂: C, 48.29; H, 3.63. Found: C, 47.81; H, 3.60.

X-ray Analysis of 5a. Orange crystals suitable for X-ray analysis were grown by slow diffusion of pentane into a CH₂Cl₂ solution of **5a**. A platelet (0.50 × 0.46 × 0.15 mm) was mounted on a glass capillary. Crystal data for C₇₃H₆₆Cl₆Fe₂O₄Pt₂ (fw 1845.76): orthorhombic, space group *P*2₁2₁2₁, cell dimensions (293 K) *a* = 14.0951(5) Å, *b* = 16.8149(6) Å, *c* = 29.3881(11) Å, and *V* = 6965.2(4) Å³ with *Z* = 4 and *D_c* = 1.760 Mg/m³, *μ* = 4.784 mm⁻¹ (Mo Kα, graphite monochromated), *λ* = 0.71073 Å, *F*(000) = 3624. The data were collected at room temperature on a Siemens SMART platform (CCD detector, detector distance 40 mm) in the *θ* range 1.39–24.71 (*ω*-scans, exposure time = 5 s). Unit cell dimensions determination and data reduction were performed by standard procedures, and an empirical absorption correction (SADABS) was applied. The structure was solved with SHELXS-96 using direct methods as described for **2a**. Of the 38772 measured reflections with index ranges -16 ≤ *h* ≤ 16, 0 ≤ *k* ≤ 19, 0 ≤ *l* ≤ 34, 11875 independent reflections (*R_{int}* = 0.0892) were used in the refinement (820 parameters, full-matrix least-squares on *F*² with anisotropic displacement parameters for all non-H atoms. Hydrogen atoms were treated as for **2a**. The absolute configuration at the P atoms was determined to be (S,S) by refinement of the Flack *x* parameter = -0.0153(65). Final residuals (*I* > 2σ(*I*)) were *R*₁ = 0.0462 and *wR*₂ = 0.0947 (all data *R*₁ = 0.0676 and *wR*₂ = 0.1029), GOF 0.985. Max. and min. difference peaks were +1.089 and -1.536 e Å⁻³; largest and mean Δ/*σ* = -0.26 and 0.017. Molecular graphics were performed with the program XP (50% ellipsoids). Atomic coordinates, anisotropic displacement coefficients, and an extended list of interatomic distances and angles are available as Supporting Information. Selected interatomic distances and angles are reported in Table 2.

[Rh(COD)((S,S)-3a)]BF₄ (6a). [Rh(COD)₂]BF₄ (66 mg, 0.163 mmol) and (S,S)-**3a** (100 mg, 0.163 mmol) are dissolved in THF (8 mL). After stirring for 2 h at room temperature, the orange solid is filtered off, washed with THF and hexane, and dried in vacuum. Yield: 120 mg (81%). ³¹P NMR (CD₂Cl₂, 162 MHz, 293 K): δ 18.9 (br, 2P); 193 K: δ 17.1 (d, ¹J_{RhP} = 153 Hz). ¹H NMR (CDCl₃, 293 K): δ 8.40–6.88 (m, 18H, ArH), 4.40–4.12 (m, 10H, 4 = CH, 6 CpH), 3.97 (s, 6H, 2 OCH₃), 3.75

(s, 2H, 2 CpH), 2.36–1.86 (m, 8H, 4 CH₂). MS (FAB⁺): *m/z* 825.1 (M⁺ – BF₄, 40), 717.0 (M⁺ – BF₄ – COD, 100). The presence of water was evidenced by IR spectroscopy (3426 cm⁻¹, br, KBr pellet) and by ¹H NMR (CDCl₃) (δ 1.58, s, 6H, 3 H₂O). Anal. Calcd for C₄₄H₄₄BF₄O₂P₂Rh·3H₂O: C, 54.68; H, 5.00. Found: C, 54.48; H, 4.90.

[Rh(COD)((S,S)-3b)]BF₄ (6b). [Rh(COD)₂]BF₄ (44 mg, 0.107 mmol) and (S,S)-**3b** (70 mg, 0.107 mmol) were dissolved in THF (5 mL). After stirring for 15 h at room temperature, the solution is concentrated under vacuum (1 mL), and Et₂O is added. The resulting yellow precipitate is filtered off, washed with Et₂O, and dried in vacuum. Yield: 80 mg (78%). ³¹P NMR (CD₂Cl₂, 162 MHz): δ 19.3 (br, 2P); 233 K: δ 19.1 (d, ¹J_{RhP} = 151 Hz). ¹H NMR (CDCl₃, 293 K): δ 8.33 (m, 2H, NpH), 8.10 (m, 2H, NpH), 7.94–7.45 (m, 20H, ArH), 4.58 (m, 4H, 4 =CH), 4.28, 4.11, 3.95, 3.75 (4 s, 8H, 2 CpH), 2.36–1.93, 1.60–1.58 (2 m, 8H, 4 CH₂). MS (FAB⁺): *m/z* 865.1 (M⁺ – BF₄, 82), 757.0 (M⁺ – BF₄ – COD, 100). The presence of water was evidenced by IR spectroscopy (3444 cm⁻¹, br, KBr pellet) and by ¹H NMR (CDCl₃) (δ 1.85, s, 6H, 3 H₂O). Anal. Calcd for C₅₀H₄₄BF₄P₂·Rh·3H₂O: C, 59.67; H, 5.01. Found: C, 59.69; H, 4.76.

Catalytic Hydrogenations. The standard procedure was as follows: the substrate (1.64 mmol) and the catalyst (according to method, see the Supporting Information) were dissolved in 10 mL of the solvent under argon. The solution was stirred for 15 min and then transferred via a steel capillary into a 180 mL thermostated glass reactor or a 50 mL stainless steel autoclave. The inert gas was then replaced by

hydrogen (three cycles), and the pressure was set. After completion of the reaction (total reaction times 15–20 h), the conversion was determined by gas chromatography, and the product was recovered quantitatively after filtration of the reaction solution on a plug of silica to remove the catalyst. The enantiomeric purity of **8** was determined by GC (L-Chirasil-Val column, on column injection). *N*-Acetylphenylalanine was converted to the methyl ester before analysis. The ee of (*R*)-*N*-methyl-*N*-acetylphenylalanine **10** was determined by HPLC (Chiracel OD-H column, eluent: hexane/*i*-PrOH, 90:10). Experimental and analytical details for all substrates are given in the Supporting Information.

Acknowledgment. A.M. thanks the Swiss National Science Foundation (CHiral 2 project) for financial support to F.M. The authors are grateful to Mrs. A. Holderer, Mrs. A. Balzer, and Mr. P. Imhof for performing the catalytic hydrogenation reactions.

Supporting Information Available: A listing of atomic coordinates, anisotropic displacement coefficients, bond distances and angles, and H atom coordinates for (S,S)-**2a** and **5a**, drawings of conformers for **6a,b**, and details of the hydrogenation reactions. This material is available free of charge via the Internet at <http://pubs.acs.org>.

OM980754A